Signal Processing 89 (2009) 244–251

Contents lists available at ScienceDirect

Signal Processing

journal homepage: www.elsevier.com/locate/sigpro

Fast communication

Joint DOD and DOA estimation for bistatic MIMO radar

Ming Jin *, Guisheng Liao, Jun Li

National Laboratory of Radar Signal Processing, Xidian University, Xi'an, Shaanxi 710071, China

ARTICLE INFO

Article history:
Received 20 March 2008
Received in revised form
21 July 2008
Accepted 18 August 2008
Available online 28 August 2008

Keywords:
ESPRIT
Bistatic MIMO radar
Direction of departure
Direction of arrival
Closed-form solution

ABSTRACT

A joint direction of arrivals (DOAs) and direction of departures (DODs) estimation algorithm for bistatic multiple-input multiple-output (MIMO) radar via ESPRIT by means of the rotational factor produced by multi-transmitter is presented. The DOAs and DODs of targets can be solved in closed form and paired automatically. Furthermore, the spatial colored noise can be cancelled in the case of three-transmitters configuration by using this method. Simulation results confirm the performance of the algorithm.

1. Introduction

A multiple-input multiple-output (MIMO) [1–8] radar has a number of potential advantages over conventional phased-array radar. By exploiting the spatial diversity, statistical MIMO radar [1,3,5], whose transmit (or both transmit and receive) antennas are spaced far away from each other, can overcome performance degradations caused by target scintillations. Unlike statistical MIMO radar, co-located MIMO radar [2,4,7,8] (to simplify, we call it MIMO radar later), whose elements in transmit and receive arrays are closely spaced, can achieve coherent processing gain. In [2], it was shown that MIMO radar allows one to obtain virtual aperture which is larger than real aperture and this results in narrower beamwidth and lower sidelobes. Parameter identifiability was also discussed in [8], which proved that the maximum number of targets that can be unambiguously identified by the MIMO radar is increasing greatly. MIMO radar ground-moving target detection was treated in [6]. In [7], adaptive techniques were applied to MIMO radar for estimating the radar cross-section (RCS) of targets. In [9], the capon-based estimation of direction of arrivals (DOAs) and direction of departures (DODs) of targets for bistatic MIMO radar was presented. However, to obtain DOAs and DODs of the targets, it is assumed that the reflection coefficient is random process in [9] and two-dimension (2-D) angle search is necessitated.

ESPRIT is a high-resolution parameter estimation technique. In [10], DOA matrix method was proposed to estimate azimuth and elevation. Several methods have also been proposed to estimate DOAs and DODs for MIMO Communication Systems. The multiple signal classification (MUSIC) method was introduced in [14] to estimate DOAs and DODs. But it needs multi-dimension search. Miao et al. [11] proposed 2-D Unitary ESPRIT to estimate DOAs and DODs. High estimation performance could be achieved under the condition of high signal-to-noise ratio (SNR). But the precondition is that the channel matrix should be estimated accurately. Furthermore, the number of DOAs and DODs that the method can estimate is limited by not only the number of transmitters but also the number of receivers.

In this paper, we present an ESPRIT-based method for bistatic MIMO radar DODs and DOAs estimation. The DOAs and DODs of targets can be solved in closed form

* Corresponding author. Tel.: +86 29 88206288; fax: +86 29 88202260.
E-mail address: mingjin141@yahoo.com.cn (M. Jin).

0165-1684/$ - see front matter © 2008 Elsevier B.V. All rights reserved.
doi:10.1016/j.sigpro.2008.08.003

and paired automatically. The number of identifiable targets is more than that of the algorithm proposed in [11]. In the case of three-transmitters configuration, the spatial colored noise can be cancelled by using this algorithm.

This paper is organized as follows. The bistatic MIMO radar signal model is presented in Section 2. In Section 3, ESPRIT method is applied to bistatic MIMO radar. Both two-transmitters configuration and three-transmitters configuration systems are considered. The closed-form solution of angles is derived. Cramer–Rao bounds (CRB) for target angle are given in Section 4. Section 5 compares the estimation performance of the two systems. Finally, Section 6 concludes the paper.

2. Bistatic MIMO radar signal model

Consider a narrowband bistatic MIMO radar system with M closely spaced transmit antennas and N closely spaced receive antennas, shown in Fig. 1. The transmit antennas transmit M orthogonal coded signals. Assume that the aperiodic autocorrelation and cross-correlation sidelobes of the signals are very low even when Doppler shift exists. The transmitted baseband coded signals are denoted by $\mathbf{s}_m \in C^{1\times K}$, where m denotes the mth transmitter and $\mathbf{s}_m \mathbf{s}_m{}^{\mathrm{H}} = K$. In this paper, a class of binary sequences with zero correlation zone (ZCZ) property [13] is utilized. The simulation in Section 4 will show that even if high Doppler shift exists, the autocorrelation and cross-correlation sidelobes are still low within the ZCZ. The Doppler frequencies have almost no effect on the orthogonality of the waveforms, i.e., these waveforms retain their orthogonality approximately for the large-scale Doppler frequencies of the targets. Therefore the variety of phase within pulses caused by Doppler frequencies can be ignored. Here, we assume that all targets locate at the neighboring range bins, i.e., all the targets are within the ZCZ, and then the sidelobes of targets in different bins can be ignored. Assume that a target is located at (φ,θ), where φ is the angle of the target with respect to the transmit array (i.e. DOD) and θ is the angle with respect to the receive array (i.e. DOA). The received data arrived at the received array through reflections of the target can be described by the expression

$$\mathbf{X} = \mathbf{a}_{\mathrm{r}}(\theta)\beta\mathbf{a}_{\mathrm{t}}^{\mathrm{T}}(\varphi)\begin{bmatrix}\mathbf{s}_1\\ \cdots\\ \mathbf{s}_M\end{bmatrix}\mathrm{e}^{\mathrm{j}2\pi f_{\mathrm{d}} t_l} + \mathbf{Z}, \quad l = 1,\ldots,L \tag{1}$$

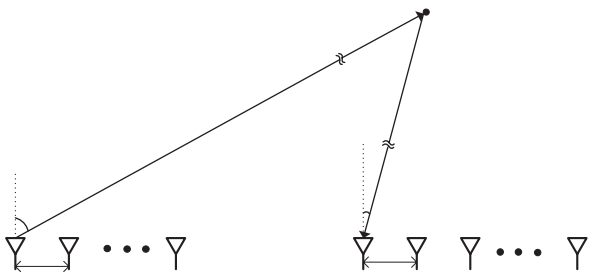

Fig. 1. Bistatic MIMO radar scenario.

where $\beta \in C$ denotes the RCS of the target and f_{d} the Doppler frequency. $\mathbf{a}_{\mathrm{r}}(\theta) \in C^{N\times 1}$ is the steering vector of the received array and $\mathbf{a}_{\mathrm{t}}(\varphi)$ is the transmit array steering vector. t_l denotes the slow time where l is the slow time index and L the number of pulses. $\mathbf{Z} \in C^{N\times K}$ denotes noise matrix and columns of $\mathbf{Z}$ are of independent and identically distributed (i.i.d) circularly symmetric complex Gaussian random vectors with zero mean and an unknown covariance matrix $\mathbf{Q}$. It should be noticed that (1) has ignored the variety of phase within pulses caused by f_{d}.

Matching the received data with the signal $\mathbf{s}_m{}^{\mathrm{H}}(\mathbf{s}_m\mathbf{s}_m{}^{\mathrm{H}})^{-1/2} = (1/\sqrt{K})\mathbf{s}_m{}^{\mathrm{H}}$, we obtain

$$\begin{aligned}\mathbf{Y}_m &= \mathbf{a}_{\mathrm{r}}(\theta)\mathbf{a}_{\mathrm{t}}^{\mathrm{T}}(\varphi)\begin{bmatrix}0\\ \cdots\\ \beta\sqrt{K}\mathrm{e}^{\mathrm{j}2\pi f_{\mathrm{d}} t_l}\\ \cdots\\ 0\end{bmatrix} + \frac{1}{\sqrt{K}}\mathbf{Z}\mathbf{s}_m^{\mathrm{H}}\\ &= \mathbf{a}_{\mathrm{r}}(\theta)a_{\mathrm{tm}}(\varphi)\beta\sqrt{K}\mathrm{e}^{\mathrm{j}2\pi f_{\mathrm{d}} t_l} + \mathbf{N}_m,\end{aligned} \tag{2}$$

where

$$\mathbf{N}_m = \frac{1}{\sqrt{K}}\mathbf{Z}\mathbf{s}_m^{\mathrm{H}} \tag{3}$$

and $a_{tm}(\varphi)$ denotes the mth element of the transmit array steering vector. $\mathbf{N}_m \in C^{N\times 1}$ denotes the noise vector after matching filter with the mth transmitted baseband signal. $(\cdot)^{\mathrm{H}}$ denotes the Hermitian transpose.

In the case of P targets, (2) can be modified to

$$\mathbf{Y}_m = \mathbf{A}_{\mathrm{r}}\mathbf{D}_m\mathbf{\Phi} + \mathbf{N}_m, \tag{4}$$

where

$$\mathbf{A}_{\mathrm{r}} = [\mathbf{a}_{\mathrm{r}}(\theta_1),\ldots,\mathbf{a}_{\mathrm{r}}(\theta_P)], \tag{5}$$

$$\mathbf{D}_m = \mathrm{diag}[a_{\mathrm{tm}}(\varphi_1),\ldots,a_{\mathrm{tm}}(\varphi_P)], \tag{6}$$

and

$$\mathbf{\Phi} = \begin{bmatrix}\beta_1\sqrt{K}\mathrm{e}^{\mathrm{j}2\pi f_{\mathrm{d}1} t_l}\\ \cdots\\ \beta_P\sqrt{K}\mathrm{e}^{\mathrm{j}2\pi f_{\mathrm{d}P} t_l}\end{bmatrix}, \tag{7}$$

where $\mathrm{diag}(\cdot)$ denotes a diagonal matrix constructed by a vector. Here, we assume that different targets have different Doppler frequencies and all the P targets are in the same range bin.

Assuming that the first transmit antenna is located at the reference origin, $\mathbf{D}_1 = \mathbf{I}_P$, where $\mathbf{I}_P$ is an identity matrix of size P.

3. Esprit method for bistatic MIMO radar

In the case of two elements at the transmit side, from (4) we can obtain

$$\mathbf{Y}_1 = \mathbf{A}_{\mathrm{r}}\mathbf{D}_1\mathbf{\Phi} + \mathbf{N}_1, \tag{8}$$

$$\mathbf{Y}_2 = \mathbf{A}_{\mathrm{r}}\mathbf{D}_2\mathbf{\Phi} + \mathbf{N}_2, \tag{9}$$

where $\mathbf{Y}_1$ and $\mathbf{Y}_2$ denote the received data from the first and the second transmitters. The covariance matrix of the

noises is as follows:

$$E[\mathbf{N}_i\mathbf{N}_j^{\mathrm{H}}] = E\left[\left(\frac{1}{\sqrt{K}}\mathbf{Z}\mathbf{s}_i^{\mathrm{H}}\right)\left(\frac{1}{\sqrt{K}}\mathbf{Z}\mathbf{s}_j^{\mathrm{H}}\right)^{\mathrm{H}}\right]$$
$$= \frac{1}{K}E\{[\mathbf{s}_i^*\otimes\mathbf{I}_M]\mathrm{vec}(\mathbf{Z})\mathrm{vec}^{\mathrm{H}}(\mathbf{Z})[\mathbf{s}_j^{\mathrm{T}}\otimes\mathbf{I}_M]\}$$
$$= \frac{1}{K}[\mathbf{s}_i^*\otimes\mathbf{I}_M][\mathbf{I}_L\otimes\mathbf{Q}][\mathbf{s}_j^{\mathrm{T}}\otimes\mathbf{I}_M]$$
$$= \begin{cases}\mathbf{Q}, & i=j\\ \mathbf{0}, & i\neq j\end{cases} \tag{10}$$

where $(\cdot)^*$, $(\cdot)^{\mathrm{T}}$, $\otimes$ and $\mathrm{vec}(\cdot)$ denote the complex conjugate, the transpose, the Kronecker matrix product and the vectorization operator, respectively. Eq. (10) shows that the cross-covariance matrix of noises is $\mathbf{0}$. This characteristic will be utilized in this paper to improve the estimate performance.

Covariance matrices of the received data can be written as follows:

$$\mathbf{R}_{11} = E[\mathbf{Y}_1\mathbf{Y}_1^{\mathrm{H}}] = \mathbf{A}_{\mathrm{r}}\mathbf{D}_1\mathbf{R}_{\mathbf{\Phi}}\mathbf{D}_1^{\mathrm{H}}\mathbf{A}_{\mathrm{r}}^{\mathrm{H}} + \mathbf{Q}, \tag{11}$$

$$\mathbf{R}_{21} = E[\mathbf{Y}_2\mathbf{Y}_1^{\mathrm{H}}] = \mathbf{A}_{\mathrm{r}}\mathbf{D}_2\mathbf{R}_{\mathbf{\Phi}}\mathbf{D}_1^{\mathrm{H}}\mathbf{A}_{\mathrm{r}}^{\mathrm{H}}, \tag{12}$$

where $\mathbf{R}_{\mathbf{\Phi}} = E[\mathbf{\Phi}\mathbf{\Phi}^{\mathrm{H}}]$. Note that if $\mathbf{Q}$ has the form $\sigma_n{}^2\mathbf{I}_N$, just as the method proposed in [10] ($\mathbf{D}_1 = \mathbf{I}_P$), we can write

$$\mathbf{R}_{11\mathrm{s}} = \mathbf{R}_{11} - \sigma_n^2\mathbf{I}_N, \tag{13}$$

$$\mathbf{R}_{21}\mathbf{R}_{11\mathrm{s}}^{\#}\mathbf{A}_{\mathrm{r}} = \mathbf{A}_{\mathrm{r}}\mathbf{D}_2, \tag{14}$$

where $\mathbf{R}_{11\mathrm{s}}^{\#}$ is the pseudoinverse of $\mathbf{R}_{11\mathrm{s}}$. It is defined same as in Eq. (22) in [10]. Since $\mathbf{D}_2$ is a diagonal matrix, we can find from (14) that diagonal elements of $\mathbf{D}_2$ and column vectors of $\mathbf{A}_{\mathrm{r}}$ make up the eigenvalues and the eigenvectors of $\mathbf{R}_{21}\mathbf{R}_{11\mathrm{s}}^{\#}$. Rank of $\mathbf{R}_{21}\mathbf{R}_{11\mathrm{s}}^{\#}$ is P, in addition. Then, we can obtain the diagonal elements of $\mathbf{D}_2$ and the columns of $\mathbf{A}_{\mathrm{r}}$ via eigendecomposition of $\mathbf{R}_{21}\mathbf{R}_{11\mathrm{s}}^{\#}$, and choosing the P nonzero eigenvalues and the corresponding eigenvectors. Thus estimation of DOAs and DODs are given through eigenvectors and eigenvalues.

However, if the noise is spatial colored, i.e., $\mathbf{Q}$ does not have the form $\sigma_n{}^2\mathbf{I}_N$, then the noise term cannot be subtracted as (13) before eigendecomposition. As a result, the estimate is biased and estimate error is large when SNR is low. To overcome these problems and avoid the estimation of the noise power, three transmit antennas configuration for bistatic MIMO radar is considered.

In the case of three transmit antennas configuration, an additional equation, i.e., the received data from the third transmitter, can be obtained from (4):

$$\mathbf{Y}_3 = \mathbf{A}_{\mathrm{r}}\mathbf{D}_3\mathbf{\Phi} + \mathbf{N}_3. \tag{15}$$

The idea of our method is to exploit the fact that the cross-covariance matrix of noises is $\mathbf{0}$ to avoid the effect of the spatial colored noise.

The covariance matrix of (8) and (15) can be written as follows:

$$\mathbf{R}_{31} = E[\mathbf{Y}_3\mathbf{Y}_1^{\mathrm{H}}] = \mathbf{A}_{\mathrm{r}}\mathbf{D}_3\mathbf{R}_{\mathbf{\Phi}}\mathbf{D}_1^{\mathrm{H}}\mathbf{A}_{\mathrm{r}}^{\mathrm{H}}. \tag{16}$$

In addition, we assume that the P targets have different θ. Then $\mathbf{A}_{\mathrm{r}}$ is full column rank and $\mathbf{A}_{\mathrm{r}}^{\mathrm{H}}\mathbf{A}_{\mathrm{r}}$ is invertible. From $\mathbf{R}_{21} = \mathbf{A}_{\mathrm{r}}\mathbf{D}_2\mathbf{R}_{\mathbf{\Phi}}\mathbf{D}_1^{\mathrm{H}}\mathbf{A}_{\mathrm{r}}^{\mathrm{H}}$ (12), we have

$$\mathbf{D}_2\mathbf{R}_{\mathbf{\Phi}}\mathbf{D}_1^{\mathrm{H}}\mathbf{A}_{\mathrm{r}}^{\mathrm{H}} = (\mathbf{A}_{\mathrm{r}}^{\mathrm{H}}\mathbf{A}_{\mathrm{r}})^{-1}\mathbf{A}_{\mathrm{r}}^{\mathrm{H}}\mathbf{R}_{21}. \tag{17}$$

By substituting (17) into (16), we obtain the following equation:

$$\mathbf{R}_{31} = \mathbf{A}_{\mathrm{r}}\mathbf{D}_3\mathbf{D}_2^{-1}(\mathbf{A}_{\mathrm{r}}^{\mathrm{H}}\mathbf{A}_{\mathrm{r}})^{-1}\mathbf{A}_{\mathrm{r}}^{\mathrm{H}}\mathbf{R}_{21}. \tag{18}$$

Thanks to the rank of $\mathbf{R}_{21} = \mathbf{A}_{\mathrm{r}}\mathbf{D}_2\mathbf{R}_{\mathbf{\Phi}}\mathbf{D}_1^{\mathrm{H}}\mathbf{A}_{\mathrm{r}}^{\mathrm{H}}$ (12) is P. Let $\{\sigma_1,\ldots,\sigma_P\}$, $\{\mathbf{u}_1,\ldots,\mathbf{u}_P\}$ and $\{\mathbf{v}_1,\ldots,\mathbf{v}_P\}$ be the P nonzero singular values, and the corresponding left and right singular vectors, respectively. Then, we obtain $\mathbf{A}_{\mathrm{r}}\mathbf{D}_2\mathbf{R}_{\mathbf{\Phi}}\mathbf{D}_1{}^{\mathrm{H}}\mathbf{A}_{\mathrm{r}}^{\mathrm{H}} = \mathbf{U}\mathbf{\Sigma}\mathbf{V}^{\mathrm{H}}$ via singular value decomposition, where $\mathbf{U} = [\mathbf{u}_1,\ldots,\mathbf{u}_P]$, $\mathbf{\Sigma} = \mathrm{diag}([\sigma_1,\ldots,\sigma_P])$ and $\mathbf{V} = [\mathbf{v}_1,\ldots,\mathbf{v}_P]$. After arranging it we get that $\mathbf{U} = \mathbf{A}_{\mathrm{r}}\mathbf{Z}$, where $\mathbf{Z} = \mathbf{D}_2\mathbf{R}_{\mathbf{\Phi}}\mathbf{D}_1^{\mathrm{H}}\mathbf{A}_{\mathrm{r}}^{\mathrm{H}}\mathbf{V}(\mathbf{V}^{\mathrm{H}}\mathbf{V})^{-1}\mathbf{\Sigma}^{-1}$ is a square matrix with size P. It is noted that both $\mathbf{U}$ and $\mathbf{A}_{\mathrm{r}}$ are full column rank, and the rank of them is P. So the square matrix $\mathbf{Z}$ is full rank. Then $\mathbf{U}$ and $\mathbf{A}_{\mathrm{r}}$ have the same column space, i.e., the left singular vectors of $\mathbf{R}_{21}$ have the same subspace as the columns of $\mathbf{A}_{\mathrm{r}}$.

We define the pseudoinverse of $\mathbf{R}_{21}$ by

$$\mathbf{R}_{21}^{\#} = \sum_{i=1}^{P}\frac{1}{\sigma_i}\mathbf{v}_i\mathbf{u}_i^{\mathrm{H}}. \tag{19}$$

Then

$$\mathbf{R}_{21}\mathbf{R}_{21}^{\#} = \left(\sum_{i=1}^{P}\sigma_i\mathbf{u}_i\mathbf{v}_i^{\mathrm{H}}\right)\left(\sum_{i=1}^{P}\frac{1}{\sigma_i}\mathbf{v}_i\mathbf{u}_i^{\mathrm{H}}\right) = \sum_{i=1}^{P}\mathbf{u}_i\mathbf{u}_i^{\mathrm{H}}$$

is orthogonal projection matrix which projects vectors onto the column space of $\mathbf{U}$ and $\mathbf{A}_{\mathrm{r}}$. Thus, we have $\mathbf{R}_{21}\mathbf{R}_{21}^{\#}\mathbf{A}_{\mathrm{r}} = \mathbf{A}_{\mathrm{r}}$. Here we constructed a matrix

$$\mathbf{R} = \mathbf{R}_{31}\mathbf{R}_{21}^{\#}. \tag{20}$$

Finally, combining (18) and (19), we obtain

$$\mathbf{R}\mathbf{A}_{\mathrm{r}} = \mathbf{R}_{31}\mathbf{R}_{21}^{\#}\mathbf{A}_{\mathrm{r}}$$
$$= \mathbf{A}_{\mathrm{r}}\mathbf{D}_3\mathbf{D}_2^{-1}(\mathbf{A}_{\mathrm{r}}^{\mathrm{H}}\mathbf{A}_{\mathrm{r}})^{-1}\mathbf{A}_{\mathrm{r}}^{\mathrm{H}}\mathbf{R}_{21}\mathbf{R}_{21}^{\#}\mathbf{A}_{\mathrm{r}}$$
$$= \mathbf{A}_{\mathrm{r}}\mathbf{D}_3\mathbf{D}_2^{-1}(\mathbf{A}_{\mathrm{r}}^{\mathrm{H}}\mathbf{A}_{\mathrm{r}})^{-1}\mathbf{A}_{\mathrm{r}}^{\mathrm{H}}\mathbf{A}_{\mathrm{r}}$$
$$= \mathbf{A}_{\mathrm{r}}\mathbf{D}_3\mathbf{D}_2^{-1}$$
$$= \mathbf{A}_{\mathrm{r}}\mathbf{D}, \tag{21}$$

where

$$\mathbf{D} = \mathbf{D}_3\mathbf{D}_2^{-1}. \tag{22}$$

Since $\mathbf{D}$ is a diagonal matrix, we obtain the diagonal elements of $\mathbf{D}$ and $\mathbf{A}_{\mathrm{r}}$ via eigendecomposition of $\mathbf{R}$ as mentioned before. Assume the eigendecomposition of $\mathbf{R}$ can be described as

$$\mathbf{R}\mathbf{\Xi} = \mathbf{\Xi}\mathbf{\Lambda}, \tag{23}$$

where $\mathbf{\Lambda} = \mathrm{diag}[\lambda_1,\lambda_2,\ldots,\lambda_P]$ represents the P nonzero eigenvalues of $\mathbf{R}$ and $\mathbf{\Xi}$ the corresponding eigenvectors. In practice, the number of nonzero eigenvalues is larger than P because of estimation error of covariance matrix and noise. Then $\mathbf{\Lambda}$ and $\mathbf{\Xi}$ are the P largest eigenvalues of $\mathbf{R}$ and the corresponding eigenvectors. Estimates of DOAs and DODs can be obtained through $\mathbf{\Xi}$ and $\mathbf{\Lambda}$, respectively.

Assume that uniform linear arrays (ULAs) are equipped at both transmit and receive sides, and take the antenna elements are spaced at distances Δ_{t} and Δ_{r}. Then the DODs

of the targets are

$$\varphi_i = \arcsin\left(\angle(\lambda_i)\frac{\lambda}{2\pi\Delta_t}\right), \quad i = 1,\ldots,P, \tag{24}$$

where $\angle(\lambda_i)$ denotes the phase of λ_i. λ denotes the wavelength.

Now we derive the closed-form solution of DOAs via least-square method. Assume $\boldsymbol{\xi}_i = \gamma_i \mathbf{a}(\theta_i)$ to be the ith column of Ξ. Then, $\hat{\mathbf{a}}(\theta_i) = (\boldsymbol{\xi}_i \gamma^*{}_i / |\gamma_i|^2)$ has the same phases as the array response vector $\mathbf{a}(\theta_i)$. Let $\boldsymbol{\Gamma}_{\text{wrap}} = \angle\hat{\mathbf{a}}(\theta_i)$ be the phase of $\hat{\mathbf{a}}(\theta_i)$. When $\Delta_r \leqslant \lambda/2$, we can unwrap the phases as follows:

$$\begin{aligned}&\boldsymbol{\Gamma}_{\text{unwrap}}(1) = \boldsymbol{\Gamma}_{\text{wrap}}(1)\\ &\boldsymbol{\Gamma}_{\text{unwrap}}(n+1) = \boldsymbol{\Gamma}_{\text{unwrap}}(n) + \delta\phi(n), \quad n = 1,\ldots,N-1\end{aligned} \tag{25}$$

where

$$\begin{aligned}&\delta\phi(m)\\ &= \begin{cases}\boldsymbol{\Gamma}_{\text{wrap}}(n+1) - \boldsymbol{\Gamma}_{\text{wrap}}(n) & \boldsymbol{\Gamma}_{\text{wrap}}(n+1) - \boldsymbol{\Gamma}_{\text{wrap}}(n) \leqslant \pi,\\ \boldsymbol{\Gamma}_{\text{wrap}}(n+1) - \boldsymbol{\Gamma}_{\text{wrap}}(n) - 2\pi & \boldsymbol{\Gamma}_{\text{wrap}}(n+1) - \boldsymbol{\Gamma}_{\text{wrap}}(n) > \pi,\\ \boldsymbol{\Gamma}_{\text{wrap}}(n+1) - \boldsymbol{\Gamma}_{\text{wrap}}(n) + 2\pi & \boldsymbol{\Gamma}_{\text{wrap}}(n+1) - \boldsymbol{\Gamma}_{\text{wrap}}(n) < -\pi.\end{cases}\end{aligned} \tag{26}$$

The unwrapped phase of array response vector $\mathbf{a}(\theta_i)$ is

$$\begin{aligned}\boldsymbol{\Gamma}^{\text{id}}_{\text{unwrap}} &= \left[0, \frac{2\pi}{\lambda}\Delta_r \sin(\theta_i), \ldots, \frac{2\pi}{\lambda}(N-1)\Delta_r \sin(\theta_i)\right]^{\mathrm{T}},\\ &= \boldsymbol{\Pi}\sin(\theta_i)\end{aligned} \tag{27}$$

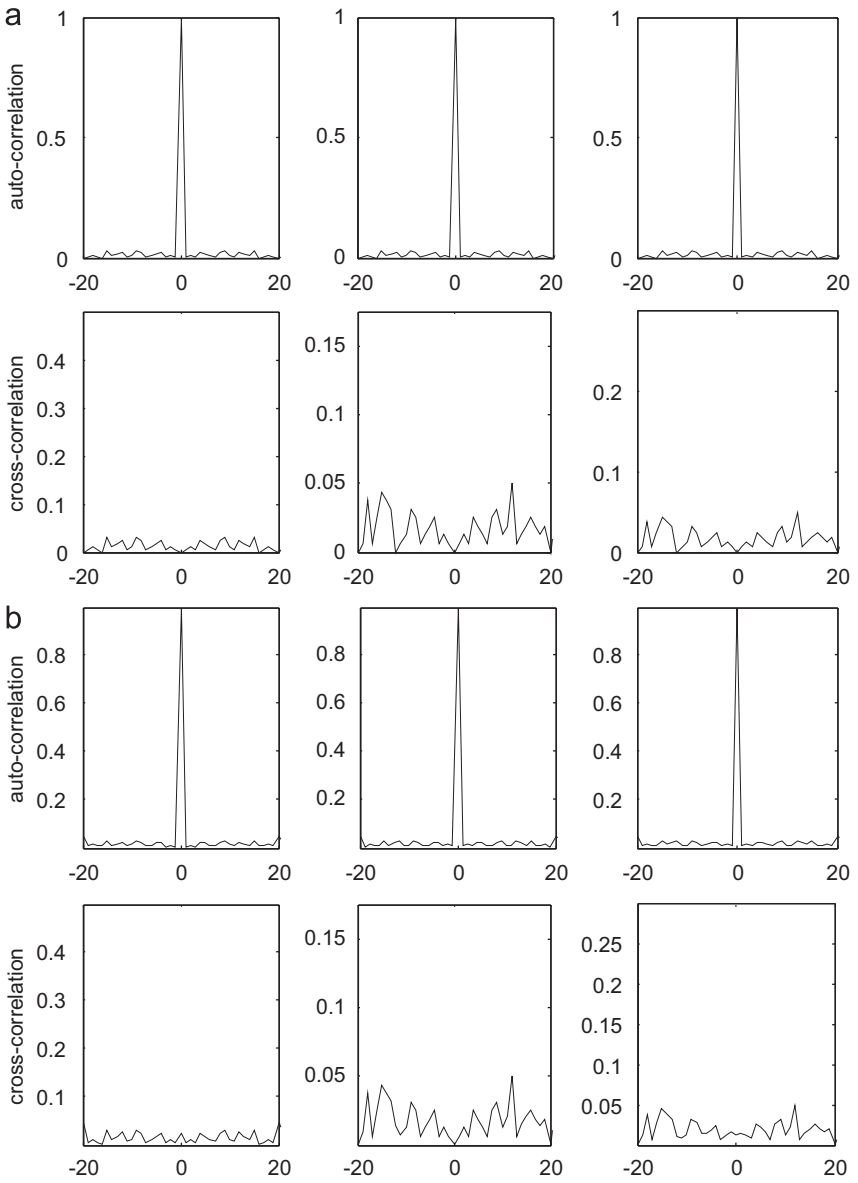

Fig. 2. The aperiodic normalized autocorrelation and cross-correlation of the transmitted waveforms within ZCZ with pulse width 10 μs: (a) no Doppler frequency and (b) Doppler frequency 5000 Hz.

where

$$\mathbf{\Pi}=\left[0,\frac{2\pi}{\lambda}\Delta_{\mathrm{r}},\ldots,\frac{2\pi}{\lambda}(N-1)\Delta_{\mathrm{r}}\right]^{\mathrm{T}}. \tag{28}$$

Then the least-square estimation of the angle is given by

$$\begin{aligned}\hat{\theta}_i&=\arg\min_{\theta}\left\|\mathbf{\Gamma}_{\mathrm{unwrap}}-\mathbf{\Pi}\sin(\theta_i)\right\|^2\\&=\arcsin\left(\frac{\mathbf{\Gamma}_{\mathrm{unwrap}}^{\mathrm{T}}\mathbf{\Pi}}{\mathbf{\Pi}^{\mathrm{T}}\mathbf{\Pi}}\right).\end{aligned} \tag{29}$$

It should be mentioned that bistatic MIMO radar can estimate as many target angles as the number of receive antennas. The DOAs and DODs of the targets are paired automatically.

4. Cramer–Rao bound

In the case of three transmit antennas configuration, the Cramer–Rao bound (CRB) of DOAs and DODs are considered here. Rewrite the received data as

$$\begin{aligned}\mathbf{Y}&=\begin{bmatrix}\mathbf{Y}_1\\\mathbf{Y}_2\\\mathbf{Y}_3\end{bmatrix}=\begin{bmatrix}\mathbf{A}_{\mathrm{r}}\mathbf{D}_1\mathbf{\Phi}\\\mathbf{A}_{\mathrm{r}}\mathbf{D}_2\mathbf{\Phi}\\\mathbf{A}_{\mathrm{r}}\mathbf{D}_3\mathbf{\Phi}\end{bmatrix}+\begin{bmatrix}\mathbf{N}_1\\\mathbf{N}_2\\\mathbf{N}_3\end{bmatrix}\\&=[\mathbf{a}_{\mathrm{t}}(\varphi_1)\otimes\mathbf{a}_{\mathrm{r}}(\theta_1),\ldots,\mathbf{a}_{\mathrm{t}}(\varphi_P)\otimes\mathbf{a}_{\mathrm{r}}(\theta_P)]\mathbf{\Phi}+\mathbf{N}\\&=\mathbf{K}(\boldsymbol{\theta},\boldsymbol{\phi})\mathbf{\Phi}+\mathbf{N}.\end{aligned} \tag{30}$$

The Fisher information matrix (FIM) with respect to $\boldsymbol{\theta}=[\theta_1,\ldots,\theta_P]$ and $\boldsymbol{\varphi}=[\varphi_1,\ldots,\varphi_P]$ can be written as

$$\mathbf{F}=\begin{bmatrix}\mathbf{F}_{11}\mathbf{F}_{12}\\\mathbf{F}_{21}\mathbf{F}_{22}\end{bmatrix}. \tag{31}$$

Note that the (i,j)th element of $\mathbf{F}_{11}$ is [12] given by

$$\begin{aligned}F(\theta_i,\theta_j)&=2\mathrm{Re}\,\mathrm{tr}\left[\left(\frac{\partial\mathbf{K}(\boldsymbol{\theta},\boldsymbol{\phi})\mathbf{\Phi}}{\partial\theta_i}\right)^{\mathrm{H}}\zeta^{-1}\frac{\partial\mathbf{K}(\boldsymbol{\theta},\boldsymbol{\phi})\mathbf{\Phi}}{\partial\theta_j}\right]\\&=2\mathrm{Re}\,\mathrm{tr}[(\dot{\mathbf{K}}_{\boldsymbol{\theta}}e_ie_i^{\mathrm{T}}\mathbf{\Phi})^{\mathrm{H}}\zeta^{-1}(\dot{\mathbf{K}}_{\boldsymbol{\theta}}e_je_j^{\mathrm{T}}\mathbf{\Phi})]\\&=2\mathrm{Re}\,[(e_i^{\mathrm{T}}\dot{\mathbf{K}}_{\boldsymbol{\theta}}^{\mathrm{H}}\zeta^{-1}\dot{\mathbf{K}}_{\boldsymbol{\theta}}e_j)(e_j^{\mathrm{T}}\mathbf{\Phi}\mathbf{\Phi}^{\mathrm{H}}e_i)]\\&=2L\mathrm{Re}\,[(\dot{\mathbf{K}}_{\boldsymbol{\theta}}^{\mathrm{H}}\zeta^{-1}\dot{\mathbf{K}}_{\boldsymbol{\theta}})_{ij}(\mathbf{R}_{\mathbf{\Phi}}^{\mathrm{T}})_{ij}],\end{aligned} \tag{32}$$

where

$$\dot{\mathbf{K}}_{\boldsymbol{\theta}}=\left[\mathbf{a}_{\mathrm{t}}(\varphi_1)\otimes\frac{\partial\mathbf{a}_{\mathrm{r}}(\theta_1)}{\partial\theta_1},\ldots,\mathbf{a}_{\mathrm{t}}(\varphi_P)\otimes\frac{\partial\mathbf{a}_{\mathrm{r}}(\theta_P)}{\partial\theta_P}\right], \tag{33}$$

$$\dot{\mathbf{K}}_{\boldsymbol{\phi}}=\left[\frac{\partial\mathbf{a}_{\mathrm{t}}(\varphi_1)}{\partial\varphi_1}\otimes\mathbf{a}_{\mathrm{r}}(\theta_1),\ldots,\frac{\partial\mathbf{a}_{\mathrm{t}}(\varphi_P)}{\partial\varphi_P}\otimes\mathbf{a}_{\mathrm{r}}(\theta_P)\right], \tag{34}$$

$$\mathbf{R}_{\mathbf{\Phi}}\triangleq\frac{1}{L}\mathbf{\Phi}\mathbf{\Phi}^{\mathrm{H}}, \tag{35}$$

and

$$\zeta=\begin{bmatrix}\mathbf{Q}&\mathbf{0}&\mathbf{0}\\\mathbf{0}&\mathbf{Q}&\mathbf{0}\\\mathbf{0}&\mathbf{0}&\mathbf{Q}\end{bmatrix} \tag{36}$$

where $\mathrm{Re}(\cdot)$ denotes the real part, e_i denotes the ith column of the identity matrix, $\mathrm{tr}(\cdot)$ denotes the trace of a matrix and $\mathbf{M}_{ij}$ denotes the (i,j)th element of $\mathbf{M}$.

Then

$$\mathbf{F}_{11}=2L\mathrm{Re}\,(\dot{\mathbf{K}}_{\boldsymbol{\theta}}^{\mathrm{H}}\zeta^{-1}\dot{\mathbf{K}}_{\boldsymbol{\theta}}\odot\mathbf{R}_{\mathbf{\Phi}}^{\mathrm{T}}). \tag{37}$$

where $\odot$ denotes Hadamard matrix product. Similarly, we obtain

$$\mathbf{F}_{12}=2L\mathrm{Re}\,(\dot{\mathbf{K}}_{\boldsymbol{\theta}}^{\mathrm{H}}\zeta^{-1}\dot{\mathbf{K}}_{\boldsymbol{\phi}}\odot\mathbf{R}_{\mathbf{\Phi}}^{\mathrm{T}}), \tag{38}$$

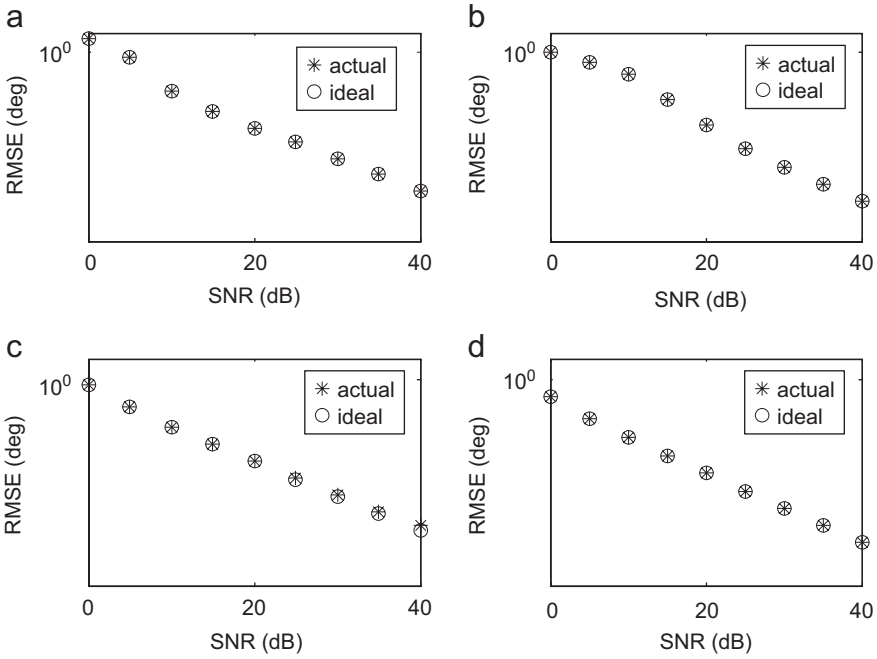

Fig. 3. The RMSE of DOD and DOA of the first target versus SNR with actual and ideal simulation data: (a) DOD with two transmitters, (b) DOA with two transmitters, (c) DOD with three transmitters and (d) DOA with three transmitters.

$$\mathbf{F}_{21} = 2L\mathrm{Re}\,(\dot{\mathbf{K}}_{\phi}^{\mathrm{H}}\zeta^{-1}\dot{\mathbf{K}}_{\theta} \odot \mathbf{R}_{\Phi}^{\mathrm{T}}), \tag{39}$$

$$\mathbf{F}_{22} = 2L\mathrm{Re}\,(\dot{\mathbf{K}}_{\phi}^{\mathrm{H}}\zeta^{-1}\dot{\mathbf{K}}_{\phi} \odot \mathbf{R}_{\Phi}^{T}), \tag{40}$$

Then the CRB matrix is

$$\mathbf{CRB} = \mathbf{F}^{-1}. \tag{41}$$

5. Simulation results

First of all, the transmitted waveforms are constructed. The start vectors $\mathbf{X}^m$ and $\mathbf{Y}^m$ in [13] are given by

$$\mathbf{X}^m = [+--+-+---++---------++-]$$

$$\mathbf{Y}^m = [-++-------+-+++-+-++-]$$

According to the method proposed in [13], a waveform set with family size 4, sequence length 160 and zero correlation zone 20 are designed. The first, third and fourth sequences are chosen as transmitted signals. The aperiodic normalized autocorrelation and cross-correlation of the transmitted waveforms within ZCZ are shown in Fig. 2. Fig. 2(a) shows the autocorrelation and cross-correlation with no Doppler shift. Fig. 2(b) shows the autocorrelation and cross-correlation with Doppler frequency 5000 Hz. The pulse width is selected as 10 μs. We find that the autocorrelation and cross-correlation sidelobes are low within the ZCZ whether Doppler frequency exists or not, i.e., the orthogonal waveform set has the characteristic of being approximately orthogonal when the Doppler frequency exists.

Computer simulations were conducted to evaluate DOD and DOA estimate performance of the proposed method in the presence of spatial colored noise. First, the effect of mutual sidelobes on estimation accuracy is evaluated. The performances of two- and three-transmitters configured systems are compared in succession. The (p, q)th element of the unknown noise covariance matrix

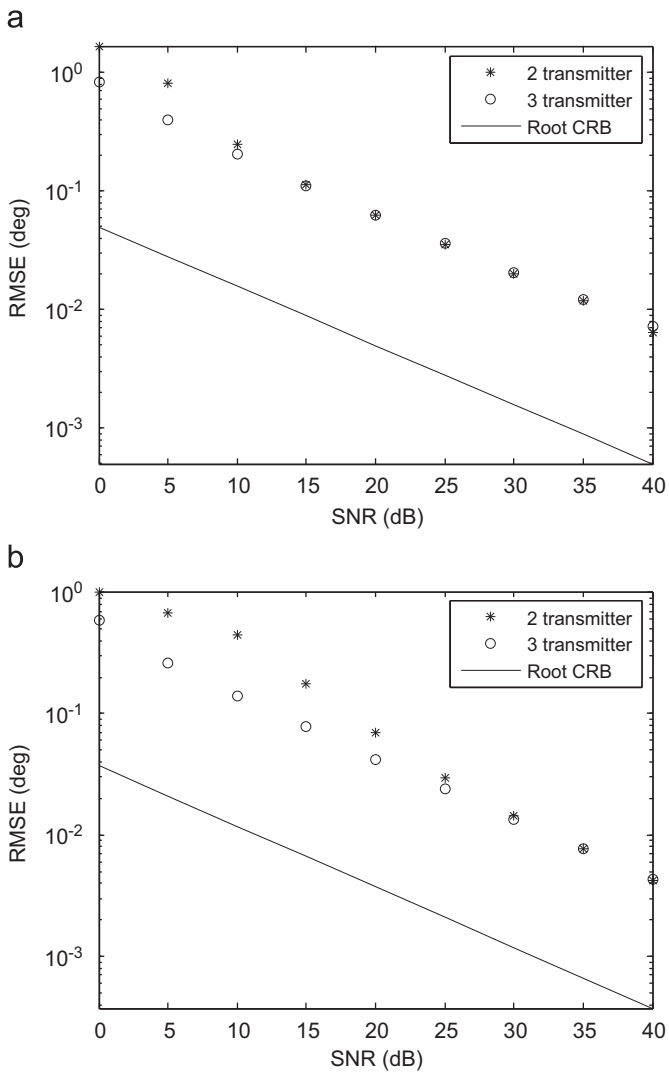

Fig. 4. RMSE and root CRB of the angles of the first target for (a) DOD and for (b) DOA.

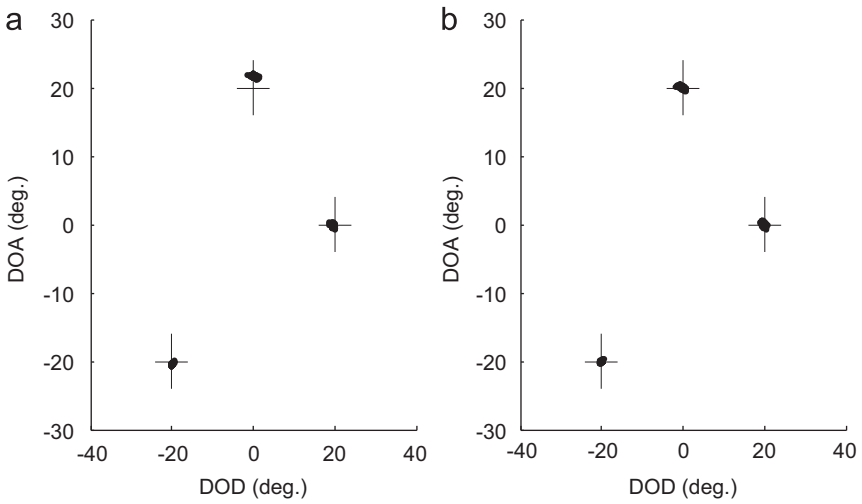

Fig. 5. The estimation result of three targets with 100 Monte Carlo trials with: (a) two-transmitters system and (b) three-transmitters system.

$\mathbf{Q}$ is $0.9^{|p-q|}e^{j((p-q)\pi)/2}$. The root-mean-square error (RMSE) of two-transmit elements bistatic MIMO radar system and three-transmit elements are compared. The RMSE is computed from $Lc = 1000$ independent trials as

$$\mathrm{RMSE} = \sqrt{\frac{1}{Lc}\sum_{i=1}^{Lc}|\hat{\theta}_i - \theta|^2}. \tag{42}$$

Assume both systems configured uniform linear arrays with half wavelength space in receiver and transmitter base. The number of the receiving elements N was chosen as 4. $P = 3$ targets locate at $(\varphi_1, \theta_1) = (-20^\circ, -20^\circ)$, $(\varphi_2, \theta_2) = (0^\circ, 20^\circ)$, $(\varphi_3, \theta_3) = (20^\circ, 0^\circ)$ and their RCSs are given by $\beta_1 = \beta_2 = \beta_3 = 1$. We also assume that different targets have different Doppler frequencies and they are 100, 2550 and 5000 Hz, respectively. The transmitted pulse width is 10 μs and the pulse repeat frequency is 10 kHz. The number of snapshots is selected as $L = 512$. Fig. 3 shows the RMSE of DOD and DOA of the first target versus SNR with actual and ideal simulation data. Here, the actual data means the mutual sidelobes exist and the ideal data have no sidelobes. It can be seen in Fig. 3 that the difference is very small.

Fig. 4 shows RMSE and root CRB of angles of the first target. From that we observe that the system with three-transmit antennas have lower RMSE than the other one when SNR is low.

Fig. 5 shows the estimation result of the three targets under the condition SNR = 10 dB. The number of Monte Carlo trials is 100. The points of intersection of dashed are actual angles of targets. Fig. 5(a) shows the result of two transmitters system. Fig. 5(b) shows the result of three-transmitters system. It is obvious that estimation of two-transmitters system is biased.

6. Conclusions

In this paper, ESPRIT method is applied to bistatic MIMO radar to estimate target angles by exploiting the rotational factor produced by multi-transmitter. The closed-form solution of DODs and DOAs is derived. The effect of sidelobes on estimate performance is very little and this is validated by computer simulation. Both two-transmitters and three-transmitters systems are considered. But theoretical analysis together with simulation results has shown that the MIMO system with three-transmit antennas outperform the system with two-transmit antennas in the spatial colored noise environment when the SNR is low. It is important to design a good waveform for MIMO. Our further work is to design better waveform set with as large a scale ZCZ as possible. To improve the estimation performance, the location method with more than three transmitters is also in process.

Acknowledgments

This research is supported by the Key Project of Ministry of Education of PR China under Contract no. 107102. The authors are grateful to four anonymous reviewers for providing them with a large number of detailed suggestions for improving the submitted manuscript.

Appendix A. Supplementary material

Supplementary data associated with this article can be found in the online version at doi:10.1016/j.sigpro.2008.08.003.

References

[1] E. Fishler, A. Haimovich, R. Blum, D. Chizhik, L. Cimini, R. Valenzuela, MIMO radar: an idea whose time has come, in: Proceedings of the IEEE Radar Conference, Newark, NJ, USA, 26–29 April 2004, pp. 71–78.
[2] I. Bekkerman, J. Tabrikian, Target detection and localization using MIMO radars and sonars, IEEE Trans. Signal Process. 54 (10) (March 2006) 3873–3883.
[3] E. Fishler, A. Haimovich, R. Blum, L. Cimini, D. Chizhik, R. Valenzuela, Spatial diversity in radars-models and detection

performance, IEEE Trans. Signal Process. 54 (3) (March 2006) 823–838.
[4] F.C. Robey, S. Coutts, D. Weikle, J.C. McHarg, K. Cuomo, MIMO radar theory and experimental results, in: Conference Record of the 38th Asilomar Conference on Signals, Systems and Computers, Lexington, MA, USA, 7–10 November 2004, pp. 300–304.
[5] E. Fishler, A. Haimovich, R. Blum, L. Cimini, D. Chizhik, R. Valenzuela, Performance of MIMO radar systems: advantages of angular diversity, in: Conference Record of the 38th Asilomar Conference on Signals, Systems and Computers, NY, USA, 7–10 November 2004, pp. 305–309.
[6] K.W. Forsythe, D.W. Bliss, G.S. Fawcett, Multiple-input multiple-output (MIMO) radar: performance issues, in: Conference Record of the 38th Asilomar Conference on Signals, Systems and Computers, Lexington, MA, USA, 7–10 November 2004, pp. 310–314.
[7] Luzhou Xu, Jian Li, P. Stoica, Target detection and parameter estimation for MIMO radar system, IEEE Trans. Aerosp. Electron. Syst., to appear.
[8] Jian Li, P. Stoica, Luzhou Xu, W. Roberts, On parameter identifiability of MIMO radar, IEEE Signal Process. Lett. 14 (12) (December 2007) 968–971.
[9] Haidong Yan, Jun Li, Guisheng Liao, Multitarget identification and localization using bistatic MIMO radar systems, EURASIP J. Adv. Signal Process. 2008 (2008) (Article ID 283483, 8pp).
[10] Q.Y. Yin, R.W. Newcomb, L.H. Zou, Estimating 2-D angle of arrival via two parallel linear array, in: IEEE International Conference on Acoustics, Speech, and Signal Processing, College Park, MD, 23–26, May 1989, pp. 2803–2806
[11] H. Miao, M. Juntti, K. Yu, 2-D unitary ESPRIT based joint AOA and AOD estimation for MIMO system, in: IEEE 17th International Symposium on Personal, Indoor and Mobile Radio Communications, Elektrobit Ltd., September 2006, pp. 1–5.
[12] P. Stoica, R.L. Moses, Spectral Analysis of Signals, Prentice-Hall, NJ, 1997 (Appendix B, pp. 285–293).
[13] P.Z. Fan, N. Suehiro, N. Kuroyanagi, X.M. Deng, Class of binary sequences with zero correlation zone, Electron. Lett. 35 (10) (1999) 777–779.
[14] Ji Li, J. Conan, S. Pierre, Joint estimation of channel parameters for MIMO communication systems, in: Second International Symposium on Wireless Communication Systems, 5–7 September 2005, pp. 22–26.